

Real-Time Linear Time-Domain Network Analysis Using Picosecond Photoconductive Mixer and Samplers

Sheng-Lung L. Huang, *Member, IEEE*, Chi H. Lee, *Fellow, IEEE*, and Hing-Loi A. Hung, *Senior Member, IEEE*

Abstract—Ion-implanted GaAs photoconductive (PC) switches have been used as an optical-microwave frequency mixer and electrical waveform samplers in a real-time sampling system. This high fidelity system has a bandwidth of 100-GHz, time resolution of 4-ps and a measurement sensitivity of $5\text{-}\mu\text{V}/\sqrt{\text{Hz}}$. Because of this high sensitivity capability, the magnitude of the testing signal can be maintained sufficiently small to allow network analysis of a device or circuit in the linear mode without signal distortion. In this paper, a linear time-domain network analysis of a broadband monolithic microwave integrated circuit (MMIC) amplifier has been demonstrated in real-time by the optoelectronic technique. A measurement time of less than 40 μs is used to acquire waveform data. The dynamic range of the system can be further improved to 40 dB by reducing the repetition rate of the step recovery diode. Since the PC switches are fabricated with processes compatible to MMIC manufacturing, this real-time system is well-suited for on-wafer MMIC characterization.

I. INTRODUCTION

CONVENTIONAL frequency-domain network analyzers have been used to measure frequency response of microwave components and MMIC's. Recently, efforts are being pursued to extend the measurement bandwidth into the millimeter-wave (MMW) frequencies with a single coaxial system. However, to achieve broadband characterizations into the high MMW regime, multiple systems (coaxial and waveguide) are still required.

Optoelectronic techniques can offer wider measurement bandwidth, and allow on-wafer MMIC characterization [1]–[5]. These techniques do not have the problems associated with the direct launch and detection of microwave/millimeter-wave signals onto MMIC's on-wafer. Real-time optical sampling can be achieved with either frequency-domain or time-domain measurement techniques. The frequency-domain approach has a limited bandwidth due to the operating frequency range of the required millimeter-wave signal source; this is the same limitation that occurs in standard electronic network analyzers. On the other hand, the time-domain measurement technique can offer a much higher bandwidth by using multi-picosecond electrical pulses as the signal source.

Manuscript received November 3, 1993; revised November 10, 1994. This work was supported by the Maryland Industrial Partnership Program.

S-L. L. Huang was with the Electrical Engineering Department, University of Maryland, College Park, MD 20742 USA. He is now with the Institute of Electro-Optical Engineering, National Sun Yat-Sen University, Kaohsiung, Taiwan, R.O.C.

C. H. Lee is with the Electrical Engineering Department, University of Maryland, College Park, MD 20742 USA.

H-L. A. Hung is with COMSAT Laboratories, Clarksburg, MD 20871 USA. IEEE Log Number 9410712.

It can be readily shown that the accuracy of S -parameter characterization does not depend on the contacting positioning of measuring probes, because only low frequency signals are needed to be detected from MMIC's. However, since each picosecond pulse transmitted to the device/circuit under test (DUT) contains a broadband frequency spectrum, time-domain measurements can result in saturating the DUT more readily than frequency-domain measurements. Therefore, the measurement sensitivity of the time-domain sampling system is critical to ensure linear characterization of the DUT. Of all the optical measurement approaches, techniques, PC sampling offers the best sensitivity [5]–[10]. One can use an input test signal of a lower magnitude for PC sampling, without the possibility of saturating the MMIC, while maintaining a good dynamic range for the measurement system. Consequently, PC technique incorporated with real-time response is more suitable for the testing of linear frequency response of MMIC's.

In sampling system, the time coherence between the test signal and the sampling signal is critical. The time coherence for standard optical pump and probe method is achieved by the beam splitting of the same optical signal. This method, however, can not perform real-time display of the sampled waveform, except at a slow measurement speed and/or short optical delay paths [11]. Other techniques would require two synthesizers with the same internal clock to synchronize the test signal and sampling signal [12]. In the present experiment, a free running microwave oscillator is phase-locked to a laser pulse train with only one synthesizer (i.e. the mode-locker for the laser). This scheme can be applied to the phase-locking of any free-running oscillator on the MMIC wafer [13]–[14].

In a present study, a PC switch was first used as an optical-microwave (OM) mixer to phase-lock a free running microwave oscillator to mode-locked laser pulse train. A step recovery diode and additional PC switches were used for signal modulation and as electronic samplers, respectively, for the characterization of a DUT. As a demonstration, this real-time waveform sampling system was used to characterize a MMIC broadband amplifier. The measured gain response was compared with that from a conventional microwave network analyzer.

II. OPTICAL-MICROWAVE PHASE LOCKING

The optical system used is a continuous wave mode-locked Nd:YLF laser which generates 50-ps pulses at a 75.7-MHz repetition rate. These laser pulses are compressed to 3 ps,

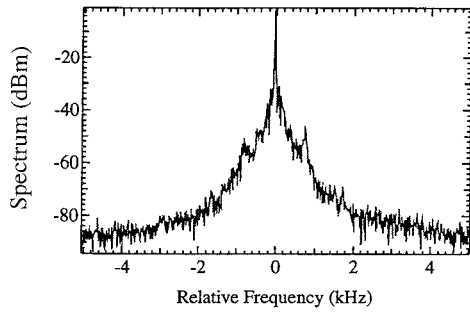


Fig. 1 Power spectrum of the frequency-doubled mode-locked laser pulse train measured at the 106th harmonic of the repetition rate (center frequency: 8 024 GHz, resolution bandwidth: 10 Hz).

which are then frequency-doubled to produce green light. The timing jitter, δT , of the green laser pulses can be calculated as follows [15]

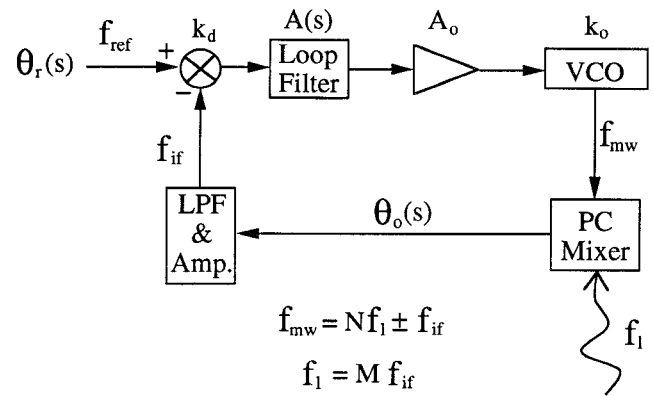
$$\delta T = \frac{1}{2\pi n f_l} \sqrt{\frac{P_n}{P_s}} \quad (1)$$

where n is the number of the harmonic, f_l is the laser repetition rate, P_s is the electrical signal power and P_n is the noise power. Fig. 1 shows the power spectrum of the green laser pulses at the 106th harmonic of its fundamental repetition rate. The root-mean-square timing jitter was estimated to be about 1 ps for a measurement time of 5 ms.

The green beam is then split into two beams, one for optical-microwave phase-locking (OMPL) and the other for waveform sampling. The time coherence between the test and sampling signals is therefore maintained. Fig. 2 is a schematic diagram of the optical-microwave phase-locked loop (OMPLL). The laser is directed to a GaAs PC switch whose substrate material has been deliberately ion-damaged to reduce the carrier lifetime. A 30-V DC is superimposed onto the output of a voltage-controlled oscillator (VCO) to bias the PC switch. This results in enhancing the signal to noise ratio (S/N) of the intermixed signal by more than 25 dB as shown in Fig. 3. The intermixed signal is then amplified through a high gain intermediate frequency (IF) amplifier. The IF phase is compared to a reference signal which is frequency divided from the laser mode-locker frequency. The resulting error signal is then delivered through a loop filter to tune the VCO. Fig. 4(a) and 4(b) shows the typical spectra of an OM phase-locked oscillator and a free running one. Once OMPL is achieved, the reference and IF waveforms can be displayed on a conventional oscilloscope, as indicated in Fig. 4(c); either one can be used as the trigger source.

For a first order approximation, the combined effect of the PC mixer and the low pass filter (LPF) provides a frequency down conversion, with a conversion factor of $\frac{1}{MN \pm 1}$. Since the bandwidth of the LPF is much wider than the loop filter, the effect of the LPF is transparent to the frequencies of interest. The closed-loop transfer function ($H(s)$) of the IF and reference frequencies can be derived as follows:

$$H(s) = \frac{\theta_0(s)}{\theta_r(s)} = \frac{k_0 k_d A_0 A(s)}{k_0 k_d A_0 A(s) + (MN \pm 1)s} \quad (2)$$



- f_{mw} : VCO frequency
- f_l : Laser repetition rate
- $\theta_r(s)$: Phase of reference frequency, f_{ref}
- $\theta_o(s)$: Phase of intermediate frequency, f_{if}
- k_d : Conversion gain of phase comparator (V/rad.)
- k_o : VCO conversion gain (rad./V-sec)
- A_o : Amplifier gain
- $A_o(s)$: Transfer function of loop filter

Fig. 2. Schematic diagram of the OMPLL.

where $A(s)$ is the transfer function of the loop filter, and it is equal to

$$A(s) = \frac{1 + sR_2C}{1 + s(R_1 + R_2)C}. \quad (3)$$

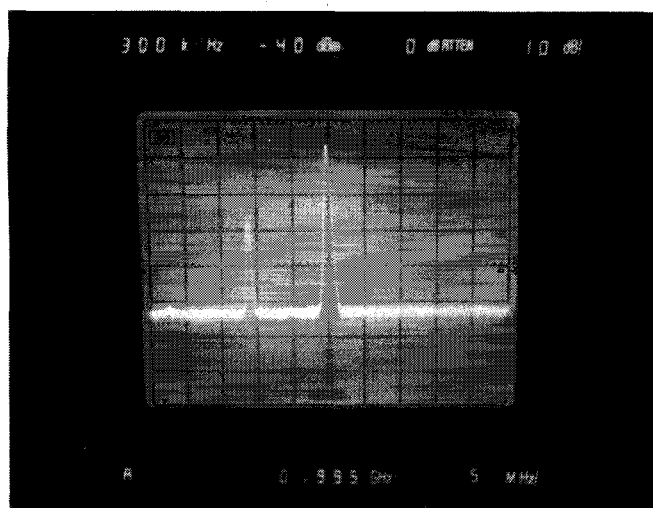
R_1 , R_2 and C are the resistances and capacitance in the loop filter. A lead-lag low-pass filter was used as the loop filter.

In order to gain a better understanding of this OMPLL, all the significant loop parameters were measured, as listed in Table I. The IF used was 4.75 MHz. Fig. 5 shows the measured frequency-to-bias conversion gain, k_o , which indicates that the change of VCO frequency is a linear function of the applied tuning voltage. It results in a linear dependence of the relative phase between the reference and intermediate signals to the tuning voltage. This capability provides an easy selection of a time window for display of the waveform.

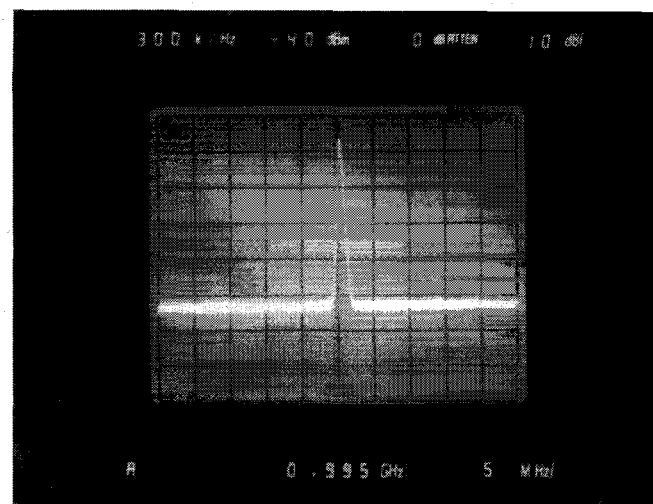
The calculated $H(s)$ for three different values of R_1 is depicted in Fig. 6 and their corresponding spectra of the phase-locked oscillator is shown in Fig. 7. Fig. 7(a) shows the best S/N obtained, which is close to that of the intermixed signal. The corresponding peak amplitude of $H(s)$ is about 2.5 dB for $R_1 = 962 \Omega$, as shown in Fig. 6 which is generally accepted as an optimum value [16]. Based on (2) and (3), the frequency of the resonance peak (ω_n) can be estimated

$$\omega_n = \sqrt{\frac{A_0 k_0 k_d}{(\tau_1 + \tau_2)(MN \pm 1)}} \quad (4)$$

where $\tau_1 = R_1 C$, $\tau_2 = R_2 C$



(a)



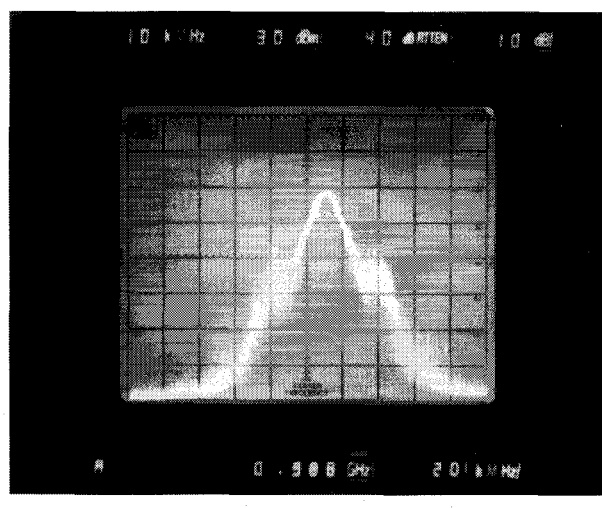
(b)

Fig. 3. (a) The intermixed signal (lefthand sideband) with 30 V DC bias. (b) The intermixed signal is smaller than the noise level of the spectrum analyzer, when there is no dc bias.

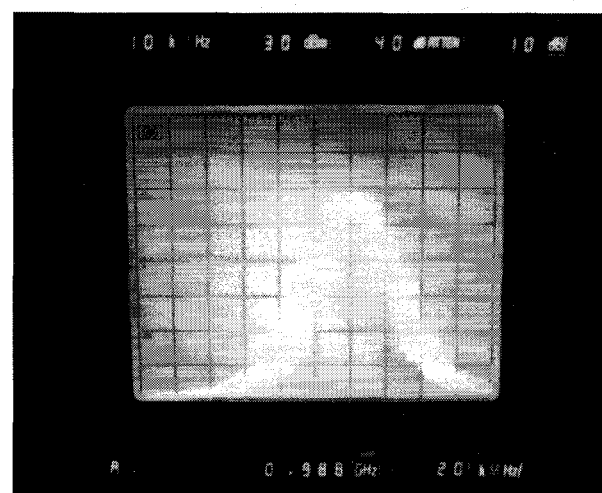
III. WAVEFORM SAMPLING

The schematic diagram of the waveform sampling system is shown in Fig. 8. After the microwave source was phase-locked to the laser pulses, the output signal was delivered to another fast PC sampling switch for waveform display. The response of the PC switch measured by the standard pump and probe PC sampling technique is shown in Fig. 9 [6]. The autocorrelated pulse width was measured to be 14.5 ps, which corresponds to an actual FWHM of 10 ps after deconvolution. The rise time of the PC response is about 3 ps which is limited by the laser pulse width. The measurement bandwidth can be calculated based on the rise time, which is more than 100 GHz [17], [18]. Since the frequency of the microwave oscillator was selected to be about 1 GHz, signals of up to the 100th harmonic of the IF should be detected to achieve a 100-GHz sampling system.

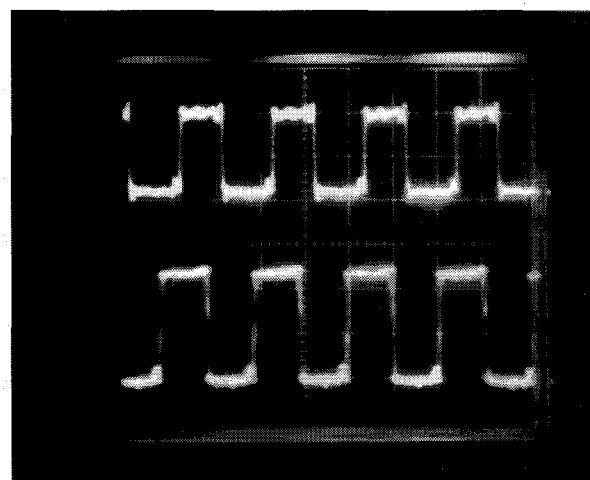
The value of the intermediate frequency (f_{if}) is based on a tradeoff between time resolution and noise. The time resolution depends on the intermediate frequency, the laser repetition rate (f_l) and the frequency of the voltage controlled microwave



(a)



(b)



(c)

Fig. 4. (a) OM phase-locked microwave oscillator spectrum; (b) free-running microwave oscillator spectrum (center frequency: 988 MHz, span: 200 kHz, resolution bandwidth: 10 kHz); (c) reference signal (4.75 MHz, trigger source, top trace), amplified and digitized intermediate frequency signal (bottom trace).

oscillator (f_{mw}), which is equal to $f_{if}/(f_{mw} \times f_l)$; therefore, a lower f_{if} value will result in better time resolution. However,

TABLE I
OMPLL PARAMETERS

A_0	0.25
R_1	$962 \Omega \sim 36.2 \text{ k}\Omega$
R_2	50Ω
C	33 nf
M	16
N	13
k_d	$-3/\pi \text{ V/rad.}$
k_0	$-2\pi \times 7.3 \times 10^6 \text{ rad./V-sec}$

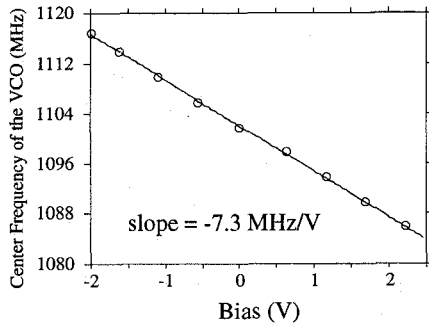


Fig. 5. Measurement of the VCO conversion gain, k_0 (slope of the curve).

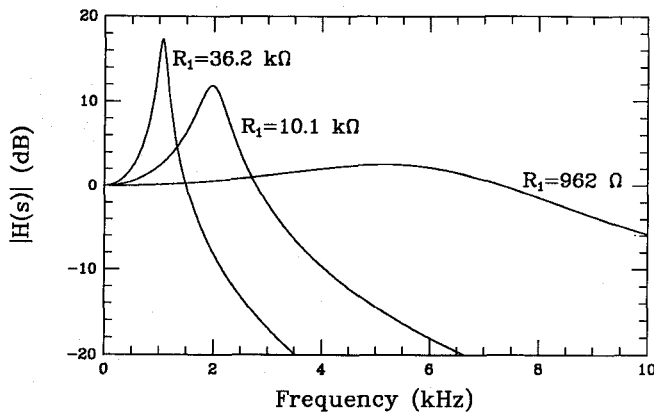


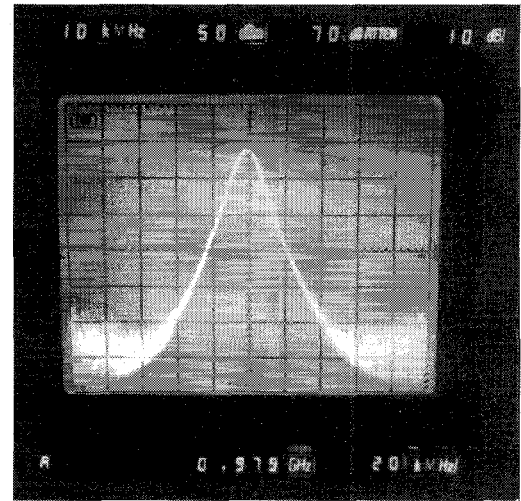
Fig. 6. Closed loop OMPLL transfer function.

when the f_{if} falls within the laser noise bandwidth, phase-locking of the source signal becomes more difficult and the resultant sampled waveform will be noisy. Low distortion is also a consideration in selecting the f_{if} . In general, the following criterion should be satisfied to avoid interference from the laser mode-locker frequency ($f_l/2$)

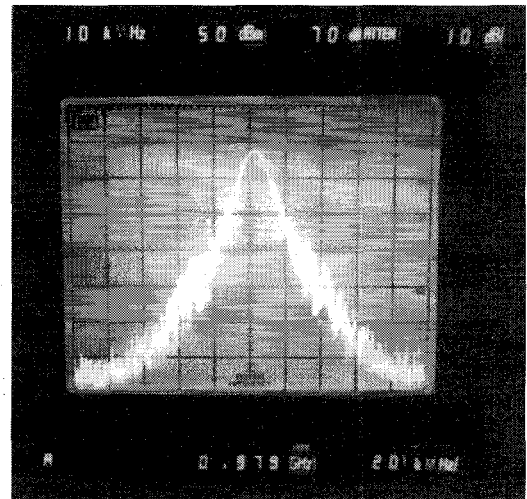
$$f_{if} < \frac{f_l f_{mw}}{2 f_{max}} \quad (5)$$

where f_{max} is the highest desired measurement frequency, which is 100 GHz in the present case.

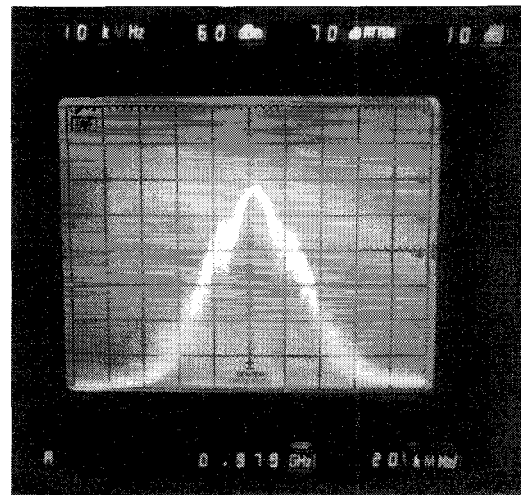
Taking the above factors into consideration, the f_{if} was selected to be 300 kHz, which corresponds to a time resolution of 4-ps. The phase-locked 1-GHz signal is shown in Fig. 10. To validate this OM sampling system, we first tested the system using a low frequency signal, which was generated by saturating the phase-locked microwave signal. The waveform



(a)



(b)



(c)

Fig. 7. Spectrum of the phase-locked oscillator for (a) $R_1 = 962 \Omega$, (b) $R_1 = 10.1 \text{ k}\Omega$, and (c) $R_1 = 36.2 \text{ k}\Omega$ (center frequency: 979 MHz, span: 200 kHz, resolution bandwidth: 10 kHz).

was measured with both a conventional sampling oscilloscope (TeK11802/SD-24, 20-GHz bandwidth) and with the present

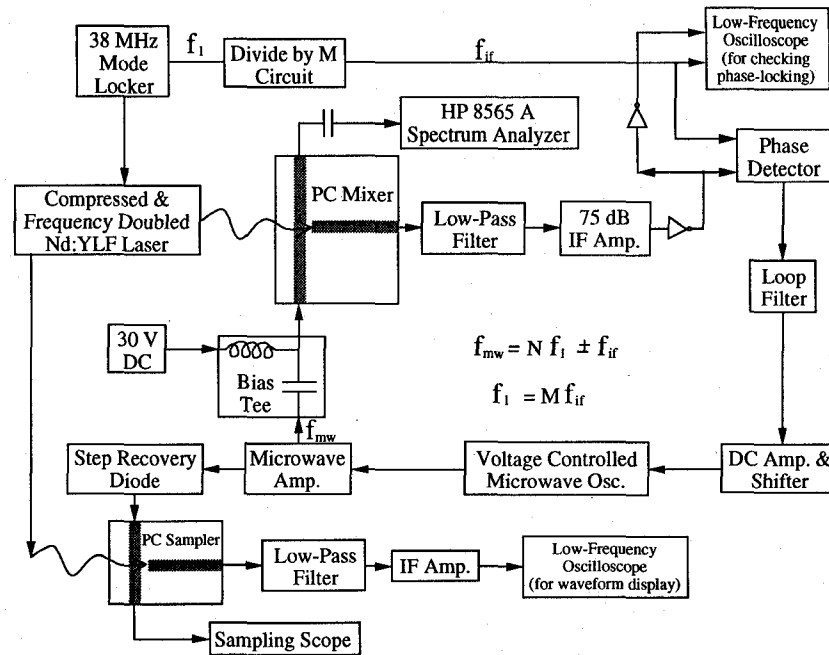


Fig. 8. Schematic diagram of the OM sampling system.

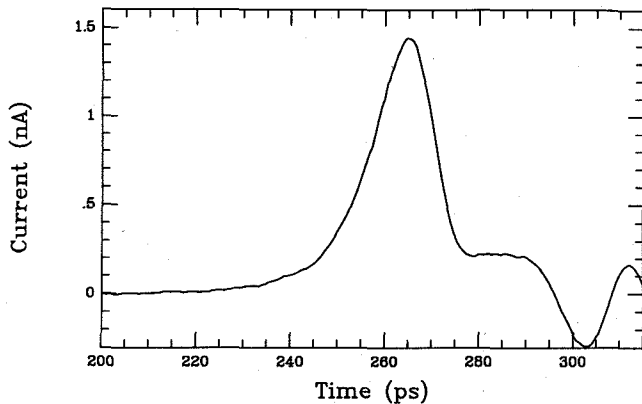


Fig. 9. Autocorrelation measurement of the PC sampler response.

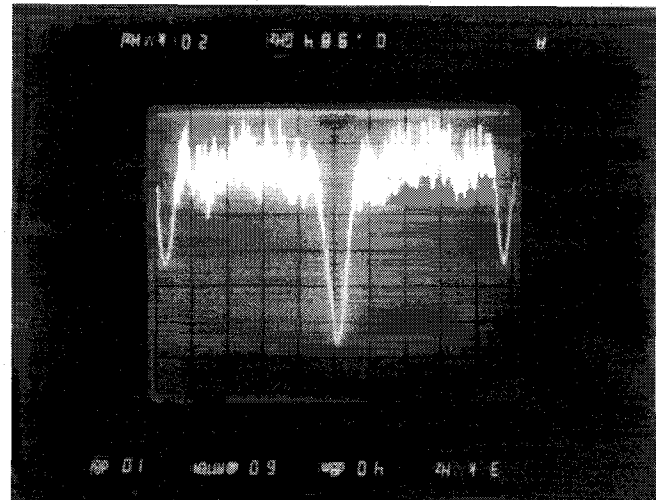


Fig. 10. Phase-locked 1-GHz signal with 300-kHz IF (center frequency: 984 MHz, span: 200 kHz, resolution bandwidth: 3 kHz).

optical system. Fig. 11 shows the comparison of the waveforms obtained by these two methods, indicating that excellent agreement was achieved.

The phase-locked microwave signal was then used to drive a step recovery diode (SRD) in order to generate high frequency signals for circuit characterization. The measured waveform is compared in real-time with that obtained from a sampling scope, as shown in Fig. 12. The OM sampling system clearly shows a faster response, as indicated in the inset of Fig. 13. To demonstrate the high sensitivity of this system, the SRD output was reduced to 200-mV magnitude, and the sampled waveform is shown in Fig. 14.

To further improve the system sensitivity, a study of noise sources was performed. We first estimated the potential noise contribution in the OMPLL. The noise was determined to originate from three sources as shown in Fig. 15. The dependence of the phase of IF, θ_0 , as a function of θ_{rn} , θ_{vcon} , and θ_{ln} , are given by the following equations [16]. For a linear system, the

superposition principle can be used to find the total θ_0

$$\left. \frac{\theta_0(s)}{\theta_{rn}(s)} \right|_{\theta_r=\theta_{vcon}=\theta_{ln}=0} = \frac{1}{1 + \frac{MN \pm 1}{k_d k_0 A_0 A(s)} \frac{1}{s}} \quad (6)$$

$$\left. \frac{\theta_0(s)}{\theta_{vcon}(s)} \right|_{\theta_r=\theta_{rn}=\theta_{ln}=0} = \frac{1/(MN \pm 1)}{1 + \frac{k_d k_0 A_0 A(s)}{MN \pm 1} \frac{1}{s}} \quad (7)$$

$$\left. \frac{\theta_0(s)}{\theta_{ln}(s)} \right|_{\theta_r=\theta_{rn}=\theta_{vcon}=0} = \frac{1/M}{1 + \frac{k_d k_0 A_0 A(s)}{MN \pm 1} \frac{1}{s}} \quad (8)$$

The measured phase noise of the mode locker, laser and VCO at 10 kHz from their center frequencies is -96 , -94 , and -82 dBc/Hz, respectively. According to (7) and (8),

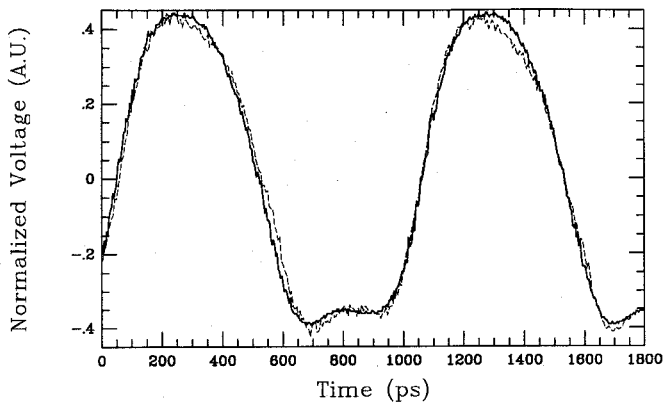


Fig. 11. Measured waveform comparison using a conventional sampling scope (solid line) and the OMPL technique (dashed line).

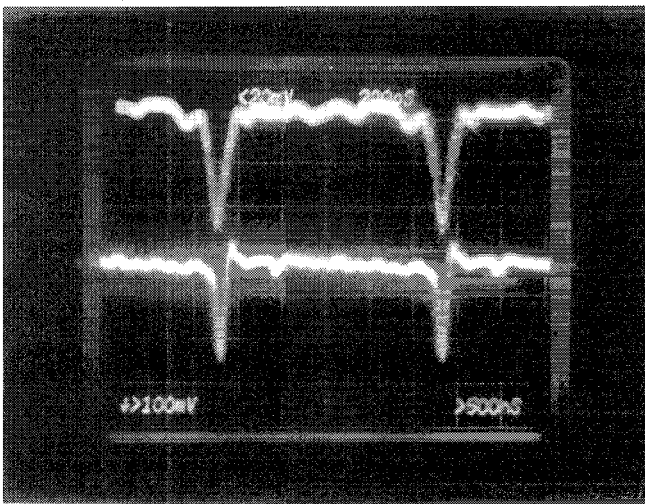


Fig. 12. Real-time display of the SRD output waveform using a sampling scope (top trace, 200 ps/div) and with the OMPL technique (bottom trace).

the noise from the VCO should be divided by a factor of $(N \pm \frac{1}{M})$ to compare the relative effect of the VCO and the laser phase noises at the IF. The equivalent VCO phase noise becomes -102 dBc/Hz and is less than the laser phase noise. In addition, since the laser phase noise is close to the mode-locker noise, we concluded that the major noise source in the phase-locked loop is from the mode-locker. When the phase-locked signal is delivered to the second PC switch, laser intensity noise (below 1 MHz) may leak through the PC switch and interfere with the IF. Depending on the amplitude of the phase-locked microwave signal, the system noise may be dominated by either mode-locker or laser intensity noise on the second PC switch. In this experiment, the sensitivity of the PC switch was measured to be about $5 \mu\text{V}/\sqrt{\text{Hz}}$, which is more than an order of magnitude more sensitive than that offered by other optoelectronic sampling techniques. The minimum detectable signal was then estimated to be about 30 mV, which is consistent with the measurement results shown in Fig. 14.

Although it is difficult to eliminate low-frequency laser amplitude noise, a high-pass filter with a cutoff frequency set at 300 kHz could be used to filter out a major portion of the laser intensity noise.

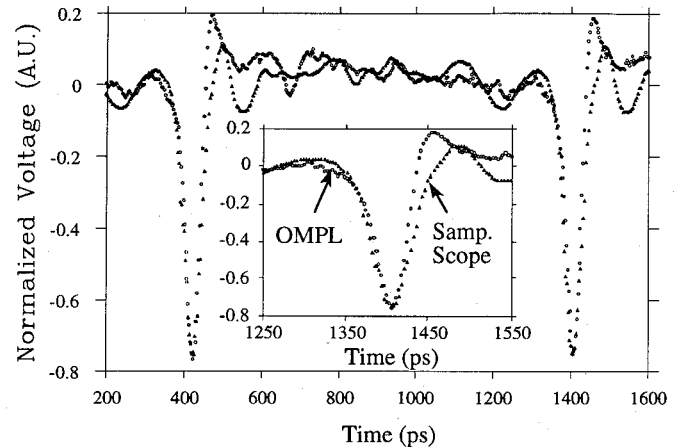


Fig. 13. Measured waveform comparison using a conventional sampling scope and the OMPL technique. Inset shows a time scale enlargement at 1400 ps.

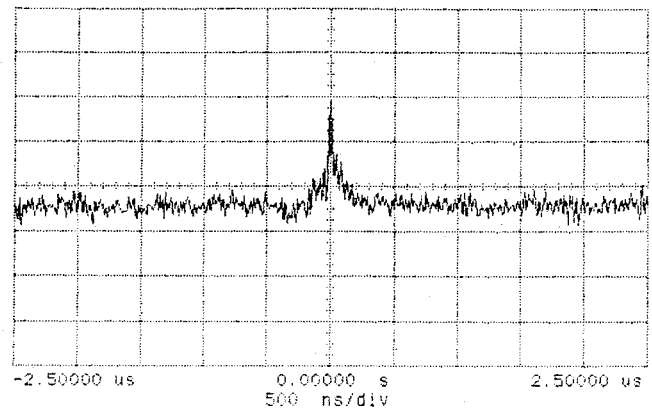
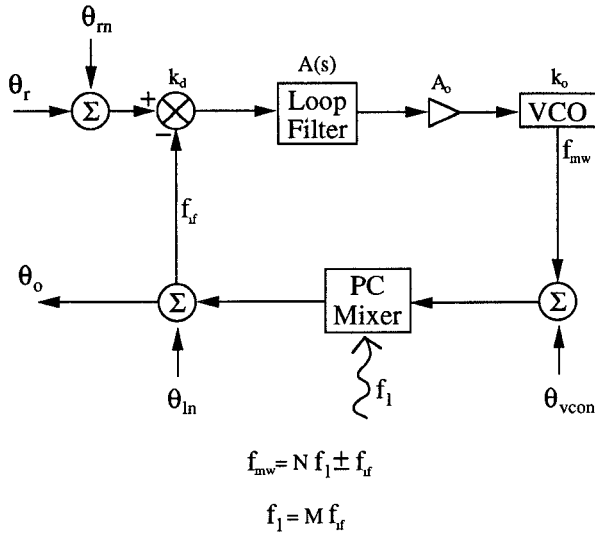


Fig. 14. Sampled waveform for a 200-mV SRD generated input signal (10 mV/div).

IV. REAL-TIME MMIC CHARACTERIZATION

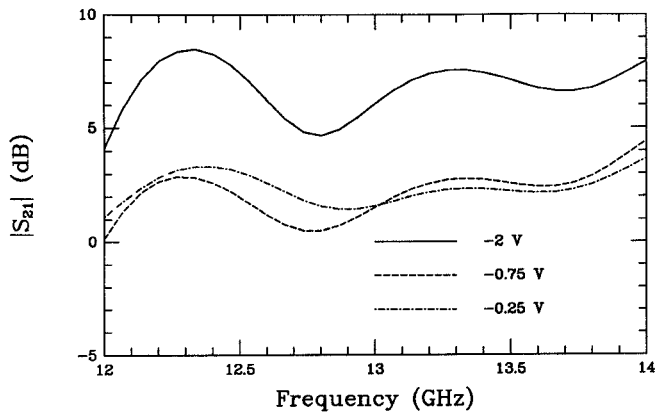
To measure the small signal S -parameter of a MMIC, the magnitude of the test signal should be small enough to prevent the device in the circuit from being saturated. The MMIC used for this experiment was a multi-stage X/Ku band amplifier with a 7-GHz bandwidth. A SRD and electronic sampling oscilloscope were used as a time-domain scalar network analyzer to determine the threshold voltage when nonlinear response of the circuit under test occurred. Fig. 16 shows the measured $|S_{21}|$ around center frequency of the MMIC's gain bandwidth with three different test signal magnitudes. A strong nonlinear response was observed for a 2-V magnitude input signal from the SRD. For the time-domain method, since the spectral response is broadband and measured at the same time, the nonlinear S_{21} amplitude may be higher than its corresponding linear S_{21} at certain frequencies due to the re-distribution of frequencies. This measurement suggested that the test signal magnitude should be kept below 1 V to avoid a nonlinear MMIC response.

Fig. 17 shows the experimental set-up of the real-time OM network analyzer. The fabrication process of the PC sampling switches are compatible with that of the MMIC.



- θ_m : Phase noise of reference frequency
- θ_{vcon} : Phase noise of VCO
- θ_{in} : Phase noise of laser repetition rate

Fig. 15. Schematic diagram of the OMPLL with noise sources.


 Fig. 16. Measured MMIC $|S_{21}|$ using a scalar time-domain network analyzer (no calibration for absolute magnitude).

The turn on resistance of the PC sampler is larger than $50 \text{ k}\Omega$; therefore, the invasive electrical effect of the PC switches in the measurement is negligible. A test signal with a 900-mV magnitude was used for this experiment. Because of the narrow bandwidth of the MMIC, the measurement of the output waveform had to extend to more than 1 ns. Therefore, the repetition rate of the input signal was reduced to about 833 MHz to cover a time-window of 1.2 ns.

Fig. 18(a) and 18(b) depicts the time domain waveforms of the input signal to the MMIC amplifier and the corresponding output signal, respectively. Eight waveforms were taken and averaged in a total data acquisition time for both input and output signal of less than $40 \mu\text{s}$. The frequency response measured using the present optical technique and the conventional frequency-domain method is shown in Fig. 19.

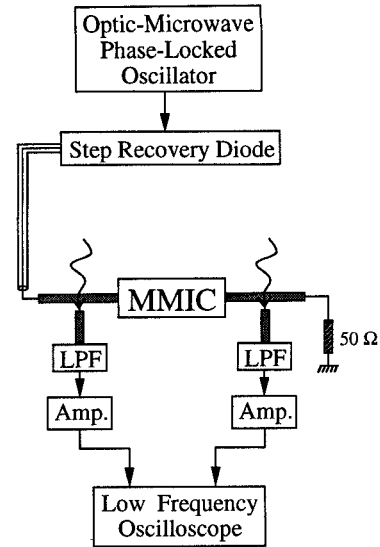


Fig. 17. Experimental setup for the real-time network analyzer.

Both techniques show similar band-pass characteristics. The present optical-microwave system provides a lower dynamic range, which can be improved as discussed below. Based on the following three facts, we can conclude that the bandwidth of the circuit under test is so narrow that if the temporal waveform of its impulse response is longer than the period of the testing impulse train, the differences in the in-band frequency response between the optical and conventional measurement techniques can increase. 1) When the temporal spread of the output waveform is short, we have very good agreement between the optical and conventional measurement techniques as shown in Fig. 11. 2) We had measured the output waveform of the MMIC using standard optical pump and probe method with low repetition rate of impulses (76 MHz), and found that the output waveform lasted more than 2 ns. Therefore, for the present real-time technique, overlapping of pulse signal among consecutive pulses did occur, which resulted in the in-band discrepancy. 3) The data shown in Figs. 18 and 19 are reproducible so that the discrepancies in Fig. 19 is not resulted from noise or lack of sensitivity. A lower repetition rate SRD could be used to eliminate the pulse overlapping. The lower dynamic range result in the out-of-band response is mainly due to the time windowing effect [6] and can be readily correct by a lower repetition rate SRD.

V. CONCLUSION

The technology involving the interaction between ultrafast optical pulses and microwave signals offers a number of potential new applications. A real-time sampling system with 100-GHz instantaneous bandwidth has been developed using optoelectronic techniques with high sensitivity, low signal distortion, minimum electrical invasiveness and picosecond time resolution. This optical system has been further enhanced to demonstrate real-time linear network analysis. The measurement of the frequency response of a broadband MMIC amplifier has been demonstrated. The time-domain data acquisition time is less than $40 \mu\text{s}$. Additional data analysis to achieve

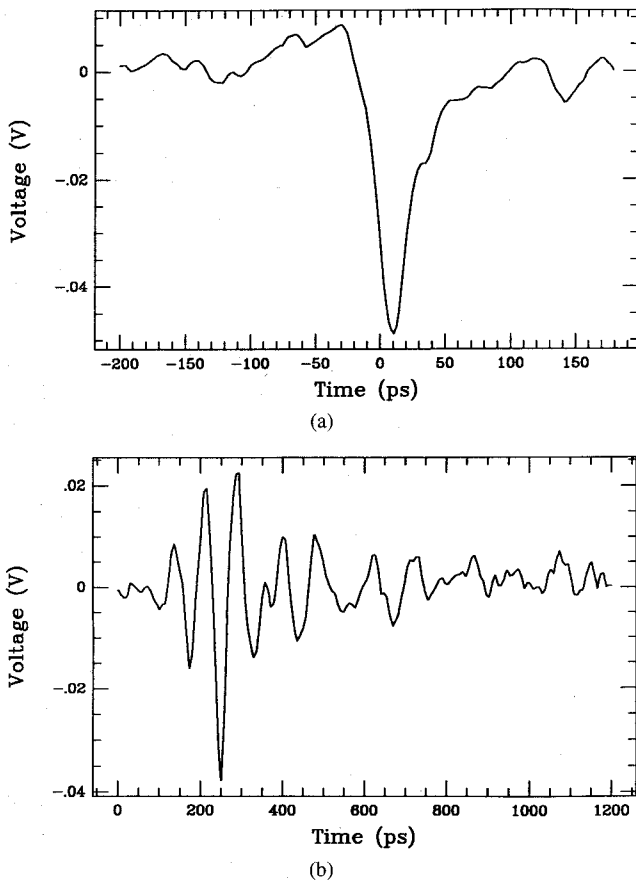


Fig. 18. MMIC (a) input, (b) output time-domain sampled waveforms.

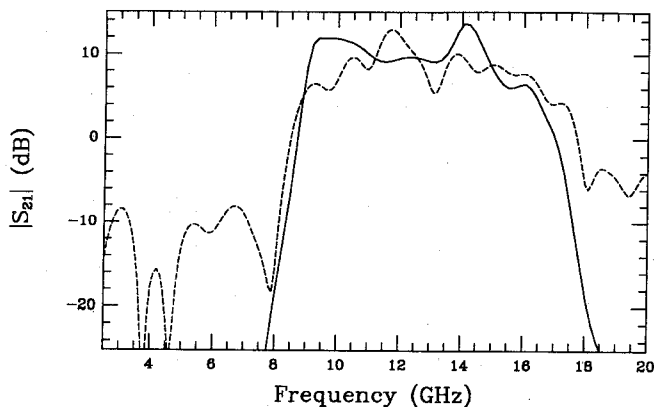


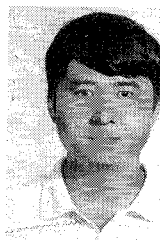
Fig. 19. Comparison of measured $|S_{21}|$ using a conventional network analyzer (solid line) and the OMPL technique (dashed line).

the frequency-domain response only requires less than a few hundred microseconds with the latest commercially available signal processing chip [19].¹ For monolithic integration of the optical test structure onto the MMIC wafer, size of the optical structure can be less than $500 \mu\text{m}$ in length to conserve valuable wafer real estate [20]. Further development of this real-time network analysis technique should provide potential applications in the microwave area.

¹The processing time for 1K FFT is 299 μs .

REFERENCES

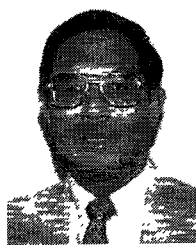
- [1] M. Matloubian *et al.*, "Wide-band millimeter wave characterization of sub-0.2 micrometer gate-length AlInAs/GaInAs," *IEEE Microwave and Guided Wave Lett.*, vol. 1, pp. 32-34, Feb. 1991.
- [2] J. A. Valdmanis and G. Mourou, "Subpicosecond electrooptic sampling: Principles and applications," *IEEE J. Quantum Electron.*, vol. QE-22, pp. 69-78, Jan. 1986.
- [3] C. H. Lee, "Picosecond optics and microwave technology," *IEEE Trans. Microwave Theory Tech.*, vol. 38, pp. 596-607, May 1990.
- [4] S. L. Huang, H.-L. A. Hung and C. H. Lee, "On-wafer optoelectronic techniques for millimeter-wave generation, control and circuit characterization," in *Ultrafast Electronics & Optoelectronics Topical Meet.*, San Francisco, CA, Jan. 1993, paper ME11.
- [5] R. B. Marcus, ed., *Measurement of High-Speed Signals in Solid State Devices*. New York: Academic, 1990, chs. 3-7.
- [6] S. L. Huang *et al.*, "On-wafer photoconductive sampling of MMIC's," *IEEE Trans. Microwave Theory Tech.*, vol. 40, pp. 2312-2320, Dec. 1992.
- [7] H.-L. A. Hung *et al.*, "Characterization of GaAs monolithic circuits by optical techniques," in *SPIE Proc. Opt. Technol. Microwave Applicat.*, Mar. 1989, vol. 1102, pp. 98-106.
- [8] M. D. Feue *et al.*, "Highly reproducible optoelectronic wafer probes with fiber input," in *Ultrafast Electron & Optoelectron. Topical Meet.*, San Francisco, CA, Jan. 1993, paper MC2.
- [9] B. H. Kolner and D. M. Bloom, "Electrooptic sampling in GaAs integrated circuits," *IEEE J. Quantum Electron.*, vol. QE-22, pp. 79-93, Jan. 1986.
- [10] R. B. Marcus *et al.*, "High-speed electrical sampling by fs photoemission," *Appl. Phys. Lett.*, vol. 49, pp. 357-359, 1986.
- [11] D. C. Edelstein, R. B. Romney, and M. Scheuermann, "Rapid programmable 300 ps optical delay scanner and signal-averaging system for ultrafast measurements," *Rev. Sci. Instrum.*, vol. 62, no. 3, pp. 579-583, Mar. 1991.
- [12] K. J. Weingarten, M. J. W. Rodwell, and D. M. Bloom, "Picosecond optical sampling of GaAs integrated circuits," *IEEE J. Quantum Electron.*, vol. 24, pp. 198-220, Feb. 1988.
- [13] M. G. Li *et al.*, "Intermixing optical and microwave signals in GaAs microstrip circuits for phase-locking applications," *IEEE Trans. Microwave Theory Tech.*, vol. 38, pp. 1924-1938, Dec. 1990.
- [14] H.-L. A. Hung *et al.*, "Characterization of microwave integrated circuits using optical phase-locking and sampling system," in *IEEE MTT-S Int. Microwave Symp.*, June 1991, paper P-6.
- [15] W. P. Robin, *Phase Noise in Signal Sources*. London: Peregrinus, 1982.
- [16] B. C. Kuo, *Automatic Control System*, 4th ed. Englewood Cliffs, NJ: Prentice-Hall, 1982.
- [17] P. M. Ferm *et al.*, "460-GHz electro-optic sampling using a nonlinear polymer film," in *Dig. Conf. Lasers and Electro-Opt.*, Anaheim, CA, May 1992, paper JFD1.
- [18] G. Mourou, W. H. Knox, and S. Williamson, "High-power picosecond switching in bulk semiconductor," in *Picosecond Optoelectronic Devices*, Chi H. Lee, Ed. Berlin: Springer-Verlag, 1984.
- [19] Alacron, i860 digital signal processing chip, model FT200/2-AT.
- [20] S. L. Huang, L. P. Golob, C. H. Lee, and H.-L. A. Hung, "A novel approach to miniature photoconductive sampling of microwave circuits," in *Dig. Conf. Lasers and Electro-Opt.*, Anaheim, CA, May 1992, paper JFD2.



Sheng-Lung L. Huang (S'88-M'93) was born in Taiwan, Republic of China, in 1964. He received the B.S. degree in electrical engineering from the National Taiwan University in 1986 and the M.S. and Ph.D. degrees from University of Maryland, College Park, in 1990 and 1993, respectively.

He is currently an associate professor of Institute of Electro-Optical Engineering at the National Sun Yat-Sen University. His research interest is in the ultrafast optoelectronics.

Dr. Huang is a member of the Optical Society of America.



Chi H. Lee (M'80–SM'86–F'91) received the B.S. degree in electrical engineering from the National Taiwan University in 1959 and the M.S. and Ph.D. degrees from Harvard University in 1962 and 1968, respectively.

He is currently a professor of electrical engineering at the University of Maryland. His research interest includes ultrafast lasers and optoelectronic devices, optical control and characterization of microwave and millimeter-wave devices and circuits.

Dr. Lee is a fellow of the Optical Society of America. He was the Chairman of the Technical Committee on Lightwave Technology of the IEEE Microwave Theory and Techniques Society. He also served as Co-Chair of the OSA Optical Meetings on Picosecond Electronics and Optoelectronics.

Hing-Loi A. Hung (S'67–M'75–SM'81), photograph and biography not available at the time of publication.